ARTICLE

Preparation and Characterization of Self-Cleaning Glass for Vehicle with Niobia Nanosheets

Ken-ichi Katsumata,*,† Sohei Okazaki,‡ Christopher E. J. Cordonier,‡ Tetsuya Shichi,‡ Takayoshi Sasaki,§ and Akira Fujishima‡,||

Materials and Structures Laboratory, Tokyo Institute of Technology, 4259 Nagatsuta, Midori-ku, Yokohama, Kanagawa 226-8503 Japan, Technology Research and Development Department, Central Japan Railway Company, 1545-33 Ohyama, Komaki City, Aichi 485-0801 Japan, International Center for Materials Nanoarchitechtonics and Nanoscale Materials Center, National Institute for Materials Science, 1-1 Namiki, Tsukuba, Ibaraki 305-0044 Japan, Kanagawa Academy of Science and Technology, KSP Building West 614 3-2-1 Sakado, Takatsu-ku, Kawasaki, Kanagawa 213-0012 Japan

ABSTRACT Self-cleaning glasses were prepared by coating niobia nanosheets and investigated on the performance. The coated glass heated at >450 °C had very low turbidity, high hardness, and excellent adhesion properties. Niobia nanosheets ($[Nb_3O_8]^-$) reacted with sodium ions (Na^+) diffused from the glass into the films to form a crystalline phase of $NaNb_3O_8$ and this phase was converted to $NaNbO_3$ at >450 °C. The films exhibited photoinduced hydrophilicity under UV irradiation but low photocatalytic oxidation activity. Excellent self-cleaning ability of the niobia nanosheet coated glass was confirmed by the Taber abrasion test, which is thought to be a candidate as self-cleaning glasses for vehicles.

KEYWORDS: photocatalyst • photoinduced hydrophilicity • self-cleaning • nanosheet • $NaNbO_3$

INTRODUCTION

Titanium dioxide (TiO_2) is a well-known photocatalyst material (1). When UV is irradiated onto TiO_2, electron and hole pairs are generated, which reduce and oxidize adsorbates on the surface, respectively, thereby producing radical species, such as OH radicals and O_2^-. These radicals can decompose most organic compounds or bacteria (2−6). Many studies have been conducted on the application of TiO_2 to water and air purification (7).

The photoinduced hydrophilicity, as well as conventional applications, of a TiO_2 photocatalyst was discovered in 1995 (8−11). When UV is irradiated onto the surface of TiO_2, a highly hydrophilic surface is generated. This surface exhibits both antifogging and self-cleaning properties, and a polycrystalline TiO_2 film coating has been applied on various industrial products, such as automobile side mirrors, window films, exterior tiles, and highway wall panels, utilizing this property (12). However, the TiO_2 film cannot apply on self-cleaning glass for vehicles. The adhesion and hardness of coated films are important factors when self-cleaning glass is applied to the windows of vehicles, because such films must be able to withstand the scrubbing action of washing brushes.

On the other hand, nanosheets are two-dimensional crystallites with high aspect ratios and flat surfaces. The flake shape has advantages in realizing of low turbidity, excellent adhesion and high hardness. Titania nanosheets are well-known to exhibit photocatalytic oxidation activity and photoinduced hydrophilicity (13, 14). This high performance as well as a highly smooth film surface has inspired the possible application of nanosheet films as a self-cleaning coating for windows. However, a dense alkaline blocking layer is necessary under titania nanosheets to avoid diffusion of alkaline components, especially sodium ion (Na^+), from the soda-lime glass during the heating process because photocatalytic activity became extremely degraded by the presence of Na^+ (15, 16). The manufacturing process, therefore, became more complicated and increased the production cost.

Recently, we reported that $NaNbO_3$ films exhibited photoinduced hydrophilic conversion under UV irradiation but poor photocatalytic oxidation activity (17). These results confirm that photoinduced hydrophilicity was induced without photocatalytic oxidation, being different from the properties observed for TiO_2. The photocatalytic activity of layered niobates (KNb_3O_8, $K_4Nb_6O_{17}$, $H_4Nb_6O_{17}$, etc.) has been studied for water splitting to H_2 production by photocatalysis and decomposition of organic compounds (18−22). They can be exfoliated to niobia nanosheets in a way similar to titania nanosheets.

* Corresponding author. Tel.: +81-45-924-5369. Fax: +81-45-924-5358. E-mail: katsumata.k.ab@m.titech.ac.jp.
Received for review February 3, 2010 and accepted March 26, 2010
† Tokyo Institute of Technology.
‡ Central Japan Railway Company.
§ National Institute for Materials Science.
|| Kanagawa Academy of Science and Technology.
DOI: 10.1021/am100091f

Published on Web 04/01/2010

With this in mind, we consider that niobia nanosheets are appropriate as the self-cleaning glass for vehicles. Because coated niobia nanosheets were expected to react with Na^+ diffused from a soda-lime glass during heating process and form $NaNbO_3$, such approaches have not been reported. In this study, we prepared $NaNbO_3$ films using niobia nanosheets having the chemical composition of $[Nb_3O_8]^-$, and investigated on the formation mechanism of $NaNbO_3$, turbidity, hardness, photocatalytic activity, and self-cleaning properties.

EXPERIMENTAL SECTION

Preparation of Coating Solution with the Layered Niobia Nanosheets. We mixed reagent-grades of potassium nitrate (KNO_3, Wako Pure Chemical Industries, Tokyo, Japan) and niobium oxide (Nb_2O_5, Wako Pure Chemical Industries, Tokyo, Japan) in a molar ratio of 2:3. After milling, the powder was heated at 1100 °C for 4 h and pulverized by a mortar. The crystalline phase formed in this sample was confirmed to be KNb_3O_8 by X-ray diffraction (XRD). The proton exchange of KNb_3O_8 was carried out in 2.0 N sulfuric acid at room temperature for 1 h with stirring and washed by ultrapure water. This proton exchange and washing processes were repeated 3 times, and K^+ ions were exchanged to H^+ or H_3O^+. The proton exchanged sample was exfoliated in 200 mL of 40 mass % tetra-*n*-butylammonium hydroxide $[CH_3(CH_2)_3]_4NOH$ (TBAOH, Sigma-Aldrich Japan K.K., Tokyo, Japan) aqueous solution (solid concentration of 5.0 mass %) at room temperature for 1 h. TBAOH was added in 2 times more molar quantity than $H^+[Nb_3O_8]^-$ ($[TBAOH]/[H^+] = 2.0$). A coating solution (1.0 mass %) was prepared by mixing the exfoliating solution and a reagent-grade ethanol (C_2H_5OH, Wako Pure Chemical Industries, Tokyo, Japan) at a volume ratio of 1:4.

Preparation of the Film on the Glass. The coating solution was spin coated on a cleaned soda-lime glass at 1000 rpm for 20 s in dry air. After coating, the film was heated at 350, 400, 450, 500, and 550 °C for 1 h in an ambient atmosphere.

Characterization. Turbidity of the films was measured by a turbidimeter (NDH 5000W, Nippon Denshoku Kogyo Co., Japan). Hardness was evaluated by a film hardness tester using pencils in conformity with JIS-K5600, which is scratch hardness test specified in the Japanese Industrial Standards (JIS). Abrasion resistance was evaluated using a Taber abrasion tester (TABER No. 410, Toyo Seiki Seisakusho Ltd., Japan) in conformity with JIS-R3212 for safety glazing materials of road vehicles. Desorption and combustion temperatures of the exfoliation agent (TBA^+) were measured by thermogravimetric analysis/differential scanning calorimeter (TGA/DSC 1, Mettler Toledo International Inc., Japan). The crystalline phases were identified by a high power XRD system (D8 DISCOVER Hybrid Super Speed, Bruker AXS, Japan) for thin film analysis, using monochromated Cu Kα radiation. The surface microstructure of the films was examined by a SEM (S-4800, Hitachi High-Technologies Co., Japan). The surface chemical composition and binding energy data of the films were evaluated by a XPS (ESCA-3400, Shimadzu Co., Japan) using Mg Kα radiation. The average surface roughness (R_a) and most difference in height (R_z) of the films were evaluated in 5 μm × 5 μm regions by an atomic force microscopy (AFM, JSPM-5200; JEOL, Japan) in the tapping mode using a conventional Si cantilever. UV−vis spectra of the films were measured using a UV−visible scanning spectrophotometer (U-3310, Hitachi High-Technologies Co., Japan).

Photocatalytic Reaction. Photocatalytic oxidation of the prepared films was evaluated by decomposition of methylene blue (MB, $C_{16}H_{18}ClN_3S$). The prepared films were immersed in 0.02 mM MB aqueous solution for 1 night to saturate the adsorption on the film surfaces. After washing by ultrapure water, a cylinder (ϕ40 × 30 mm) was contacted on the film surface by using silicone grease and 0.01 mM MB aqueous solution was poured into the cylinder. Irradiating overhead UV light, the absorption spectra of MB were measured by a UV−vis spectrophotometer. Photoinduced hydrophilicity of the films was evaluated from the water contact angle value using a commercial automatic contact angle system (OCA 15plus, dataphysics Instruments GmbH, Germany) under UV (1.0 mW/cm^2) irradiation utilizing a black light blue (BLB) lamp. The water droplet size used for the measurements was 1.0 μL. The values of water contact angle were an average of three point measurements. The superhydrophilic maintenance property of the films was evaluated from the water contact angle. After irradiating UV light adequately, the films set in desiccators in the dark.

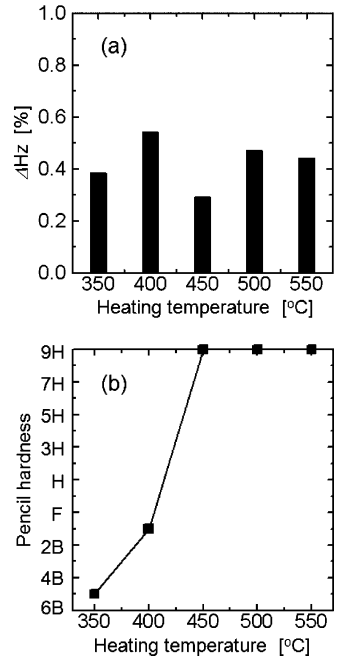

FIGURE 1. Relationship between (a) the turbidity (ΔHz) or (b) hardness of the coated glasses and heat treatment temperatures.

RESULTS AND DISCUSSION

The turbidity and hardness of the coated glasses are shown in Figure 1. The turbidity of the glasses was represented by haze value (ΔH_z). The obtained values were <0.6 regardless of heating temperatures (Figure 1a). All glasses have good optical transparency with similar to commercially available functional glasses. However, hardness of the film coated on the glass surfaces changed depending on the heating temperature as shown in Figure 1b. The hardness greatly increased by heat treatment at ≥450 °C. Similar temperature tendency was also obtained for the abrasion resistance. The films heated at 300 and 350 °C disappeared after the Taber abrasion test. The adhesion strengths between the films and glasses in these samples are poor. The films heated at 450, 500, and 550 °C remained after the Taber abrasion test and only a slight change of the ΔH_z values before and after the test. These results indicate that the films have an excellent surface hardness and abrasion resistance when heated at higher than 450 °C.

The thermogravimetric and differential scanning calorimetric (TG-DSC) curves of the powder sample, drying the coating solution at 80 °C, are shown in Figure 2. Both

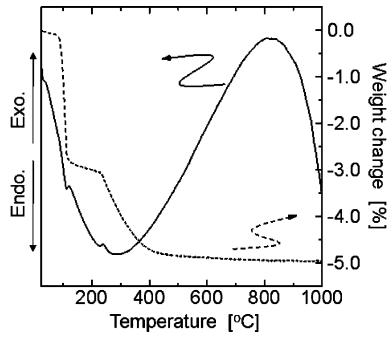

FIGURE 2. TG-DSC curves of the powder sample that dries a coating solution at 80 °C.

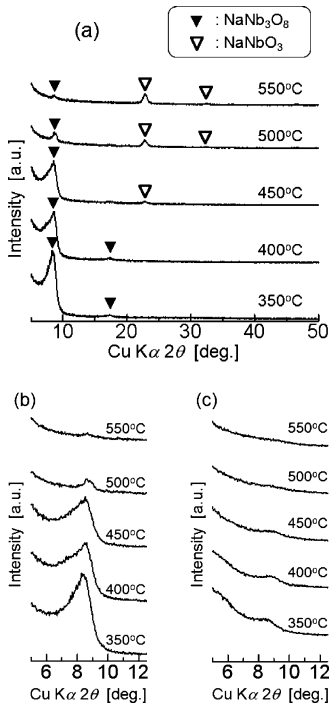

FIGURE 3. XRD patterns of the coated glasses with various heat treatment temperatures: (a) wide scan 5−50°, (b) detailed scan corresponding to the (010) reflection of $NaNb_3O_8$, (c) detailed scan of the samples prepared on the silica glass substrate.

endothermic and exothermic peaks were observed at 100 and 250 °C, respectively. Because the endothermic peak accompanied weight loss, it is attributed to the dehydration of water remained in the sample. The exothermic peak was observed with a continuous weight loss ranging from 250 to 400 °C. Thus, this peak is attributed to the thermal decomposition of the exfoliation agent (tetra-*n*-butylammonium: TBA^+).

Figure 3 shows the X-ray diffraction (XRD) patterns of the films. The crystalline phases detected in the films were $NaNb_3O_8$ and $NaNbO_3$ with *Pmnm* and *Pbcm* space groups, respectively (Figure 3a). With increasing heating temperature, the intensities of $NaNb_3O_8$ reflections became lower while $NaNbO_3$ reflections started to be observed in the samples heated at ≥450 °C, indicating conversion of $NaNb_3O_8$ to $NaNbO_3$ at those temperatures. Figure 3b shows the XRD patterns featuring the (010) reflection of $NaNb_3O_8$. The peaks shifted to higher angle with higher heating temperature. This is considered that layer spacing of $NaNb_3O_8$

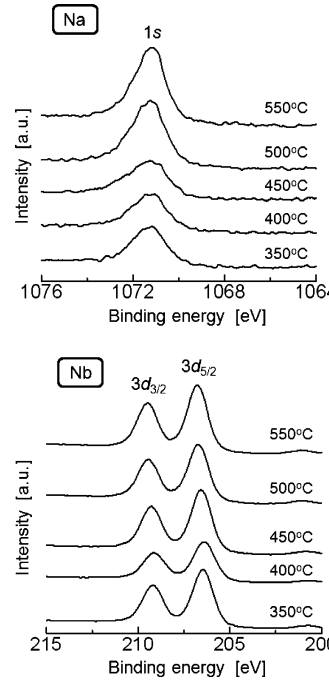

FIGURE 4. Respective XPS spectra of the Na 1s and Nb 3d regions, as acquired from the coated glasses with various heat-treatment temperatures.

was decreased by the thermal decomposition of TBA^+. Figure 3c shows the XRD patterns on the silica glass substrate. The peaks on silica glass were very broad, suggesting to being difficult to maintain a layered structure ($[Nb_3O_8]^-$) at these temperatures. In the case of soda-lime glass (Figure 3b), the peaks clearly appeared. It is guessed that the layered structure on the soda-lime glass is maintained by the existence of Na^+.

Figure 4 shows the high-resolution X-ray photoelectron spectroscopy (XPS) spectra of the Na 1s and Nb 3d regions of the film samples calibrated using C 1s (284.5 eV). The intensity of the Na 1s increased with increasing heating temperature. This change is suggested to occur according to the diffusion of Na^+ from the glass into the film. The binding energies of Nb $3d_{3/2}$ and $3d_{5/2}$ increased with increasing heating temperature. It is guessed that the binding energy of Nb−O increases since Nb−O bond lengths of $NaNbO_3$ (23) are shorter than those of $NaNb_3O_8$ (24). The binding energy of Nb $3d_{5/2}$ of the sample heated at 550 °C was in good agreement with $NaNbO_3$ (25). This result indicates that $NaNb_3O_8$ formed at lower temperatures under low Na^+ concentration changed to $NaNbO_3$ with higher Na^+ concentration with higher heating temperature.

The structure change from niobia nanosheets to $NaNbO_3$ by heat treatment is summarized in Scheme 1. Before heating, niobia nanosheets have TBA^+ in the interlayers and $TBA[Nb_3O_8]$ units maintained until about 400 °C. With increasing heating temperature, TBA^+ ions were decomposed, and Na^+ intercalated into the interlayers. If TBA^+ ion is assumed as a spherical shape, the radius calculated from the *n*-butylamine length is 0.853 nm (26, 27) and is much larger than ionic radius of Na^+ (0.116 nm) (28). Therefore, the (010) reflection shifted to higher angle with exchanging

Scheme 1. Schematic Illustration of the Structural Transformations of the Coated Niobia Nanosheets with Various Heat Treatment Temperatures

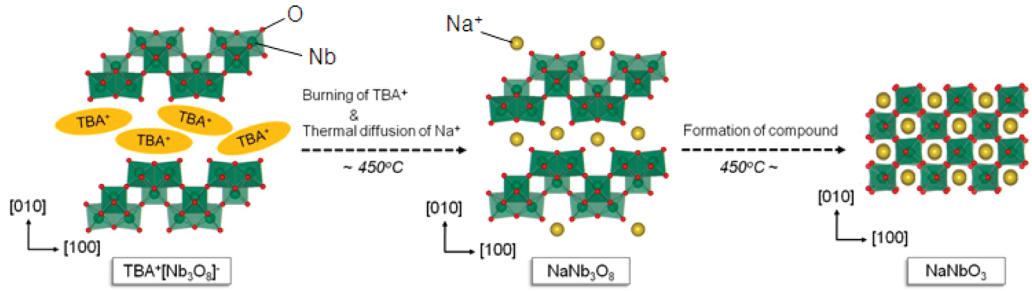

of the interlayer cations from TBA^+ to Na^+, forming $NaNb_3O_8$ (Figure 3b). At higher than 450 °C, the $NaNb_3O_8$ converted to $NaNbO_3$. The structures of niobia nanosheets ($[Nb_3O_8]^-$) and $NaNb_3O_8$ are both constructed by distorted NbO_6 octahedral units sharing the edges and corners. Three NbO_6 octahedra are connected by sharing corners and edges along the [001] direction in the niobia nanosheets. In the $NaNbO_3$ structure, NbO_6 octahedral units are connected with sharing corners along the [100], [010], and [001] directions.

Figure 5 shows the SEM photographs of the film surfaces. For the films heated at 350 and 400 °C, homogeneous microstructures, which are consisted of niobia nanosheets, were observed. By contrast, cubic shaped grains attributed to $NaNbO_3$ were observed in the films heated at 450, 500, and 550 °C, and their average grain sizes were ca. 50 nm. The boundaries observed in the microstructures are corresponded to the niobia nanosheets and the $NaNbO_3$ grains formed in the nanosheets. The R_z values (5−47 nm) of the films were larger than the R_a values (1−4 nm), and the values became larger with increasing heat treatment temperature.

Figure 6 shows changes of the water contact angle (θ) of the films as a function of UV irradiation time. The initial contact angles of the films were somewhat different among the films. The reason may be attributed to the difference of the dark storage times in the vacuum desiccators because the surfaces of the films were slowly converted to a hydrophobic state. When UV was irradiated on the films, the contact angles began to decrease. The contact angles of all films became $\theta < 5°$ after irradiation for 300 min, which is corresponding to highly hydrophilic state. This result indicates that all films exhibit the photoinduced hydrophilicity under UV irradiation. The films heated at 450, 500, and 550 °C showed higher hydrophilicizing rate than those at 350 and 400 °C, indicating higher hydrophilic conversion property in $NaNbO_3$ than $NaNb_3O_8$. Thus, the films heated at 450, 500, and 550 °C exhibited photoinduced hydrophilicity even after the Taber abrasion test.

The hydrophilic maintenance property in the dark is then shown Figure 7. The 350, 400, and 450 °C films were kept the hydrophilic state (water contact angle <5°) for 7 days. The 500 and 550 °C films were kept water contact angle <10 and 15° for 7 days, respectively. It is indicated that the films heated at lower temperature can keep highly hydrophilic state compared with those at higher temperature.

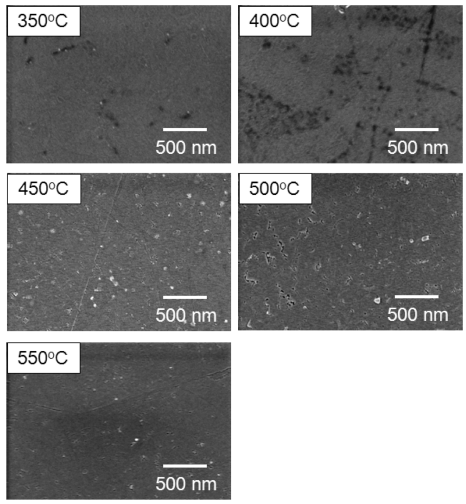

FIGURE 5. SEM photographs of the film surfaces heated at 350, 400, 450, 500, and 550 °C. The acceleration voltage was 1.0 kV.

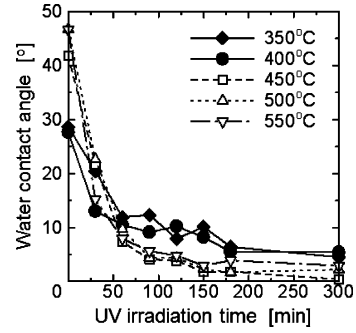

FIGURE 6. Variation of water contact angle on the films under UV irradiation. Values of the water contact angles were averages of three measurements. The light intensity was 1.0 mW/cm².

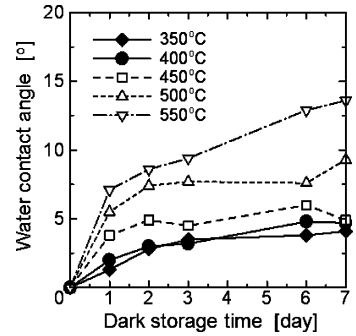

FIGURE 7. Variation of water contact angle on the films during dark storage. Values of the water contact angles were averages of three measurements.

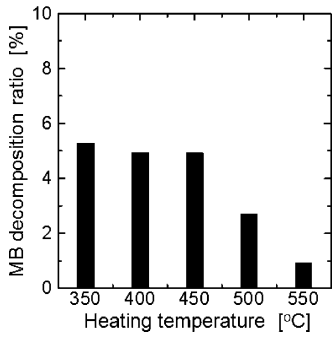

FIGURE 8. Ratio of methylene blue (MB) decomposed on the films under UV irradiation after 24 h. The light intensity was 1.0 mW/cm^2.

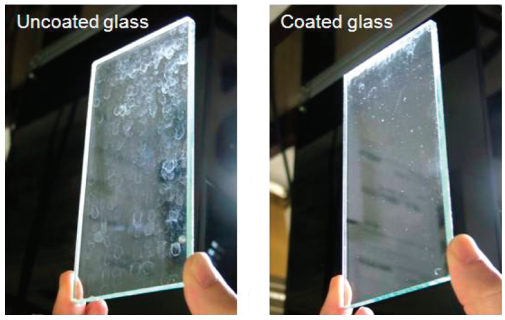

FIGURE 9. The appearance photograph of the glasses coated or uncoated the niobia nanosheets after self-cleaning test. The coated glass was heated at 450 °C for 1 h. Both glasses were irradiated by artificial sunlight lamp and sprayed with the droplet of industrial water at regular time intervals.

As shown in Figure 8, the methylene blue (MB) decomposition ratios of the films by the photocatalytic oxidation under UV irradiation were less than 6%. The ratios decreased with increasing heating temperature, and dramatically reduced by heating at 500 and 550 °C. This result indicates that $NaNb_3O_8$ and $NaNbO_3$ have low photocatalytic oxidation activities, which are compatible with the previous report (17, 29).

In the present samples, the crystalline phases of the films changed by heating temperature. Thus, the band gap energies are considered to change according to those crystalline phases. However, the observed UV−vis absorption edges of the films were almost the same with irrespective to the crystalline phases. Therefore, we consider that $NaNbO_3$ has higher photoinduced hydrophilicity compared to $NaNb_3O_8$ but lower photocatalytic oxidation activity.

Figure 9 shows photographs of the glasses with and without coating of niobia nanosheets after the self-cleaning test. The coated glass was heated at 450 °C for 1 h. Both glasses were irradiated by artificial sunlight lamp with spraying the water droplets at regular time intervals. In the case of the uncoated glass, a water scale adhered onto the glass surface, whereas no water scale adhered onto the coated glass. We also obtained similar results after the test using some simulated powders, which are including some components (C, SiO_2, Fe_2O_3, Al_2O_3, CaO, MgO, TiO_2), and little degradation of the performance was indicated after the Taber abrasion test. By contrast, the same self-cleaning test for some commercially available photocatalytic glasses indicated clear degradation of the performance. This difference is obtained not only by the photoinduced hydrophilicity but also by the flat surfaces due to the nanosheet coating, which realized the excellent adhesion and hardness of the coated films.

As long as the photoinduced hydrophilicity is maintained for the film, it shows self-cleaning ability even without the photocatalytic oxidation activity. We consider that the 450 and 500 °C films are suitable as the self-cleaning glass for vehicles with the excellent adhesion, hardness, and hydrophilic maintenance properties.

CONCLUSIONS

Glasses with self-cleaning performance were prepared by coating niobia nanosheets, and its physical properties (hardness), photocatalytic activity, and self-cleaning performance were investigated. The glasses showed good optical transparency and hardness by heating at ≥450 °C. These results are attributed to the crystalline phase change from $NaNb_3O_8$ to $NaNbO_3$. The resulting coating glasses exhibited photoinduced hydrophilicity under UV irradiation but low photocatalytic oxidation activity. Self-cleaning performance of these glasses was excellent and suitable as self-cleaning glass for vehicles.

Acknowledgment. The authors are grateful to Prof. K. Okada of Tokyo Institute of Technology for critical reading and editing of the manuscript. The authors thank Mr. Tachiyanagi, Mr. Kobune, and Ms. Hattori for their help with XRD, XPS, decomposition of methylene blue, and water contact angle measurements.

REFERENCES AND NOTES

(1) Fujishima, A.; Honda, K. *Nature* **1972**, *238*, 37.
(2) Kawai, T.; Sakata, T. *Nature* **1980**, *286*, 474.
(3) Schwitzgebel, J.; Ekerdt, J. G.; Gerischer, H.; Heller, A. *J. Phys. Chem.* **1995**, *99*, 5633.
(4) Sunada, K.; Watanabe, T.; Hashimoto, K. *J. Photochem. Photobiol. A: Chem.* **2003**, *156*, 227.
(5) Sunada, K.; Kikuchi, Y.; Hashimoto, K.; Fujishima, A. *Environ. Sci. Technol.* **1998**, *32*, 726.
(6) Trapalis, C. C.; Keivanidis, P; Kordas, G.; Zaharescu, M.; Crisan, M.; Szatvanyi, A.; Gartner, M. *Thin Solid Films* **2003**, *433*, 186.
(7) Mills, A.; LeHunte, S. *J. Photochem. Photobiol. A: Chem.* **1997**, *108*, 1.
(8) Wang, R.; Hashimoto, K.; Fujishima, A.; Chikuni, M.; Kojima, E.; Kitamura, A.; Shimohigoshi, M.; Watanabe, T. *Nature* **1997**, *388*, 431.
(9) Wang, R.; Hashimoto, K.; Fujishima, A.; Chikuni, M.; Kojima, E.; Kitamura, A.; Shimohigoshi, M.; Watanabe, T. *Adv. Mater.* **1998**, *10*, 135.
(10) Wang, R.; Sakai, N.; Fujishima, A.; Watanabe, T.; Hashimoto, K. *J. Phys. Chem. B* **1999**, *103*, 2188.
(11) Watanabe, T.; Nakajima, A.; Wang, R.; Minabe, M.; Koizumi, S.; Fujishima, A.; Hashimoto, K. *Thin Solid Films* **1999**, *351*, 260.
(12) Fujishima, A.; Hashimoto, K.; Watanabe, T. *TiO_2 Photocatalyst, Fundamentals and Applications*; BKC Inc.: Tokyo, 1999; p 66.
(13) Sakai, N.; Fukuda, K.; Shibata, T.; Ebina, Y.; Takada, K.; Sasaki, T. *J. Phys. Chem. B* **2006**, *110*, 6198.
(14) Shibata, T.; Sakai, N.; Fukuda, K.; Ebina, Y.; Sasaki, T. *Phys. Chem. Chem. Phys.* **2007**, *9*, 2413.
(15) Paz, Y.; Luo, Z.; Rabenberg, L.; Heller, A *J. Mater. Res.* **1995**, *10*, 2842.
(16) Paz, Y.; Heller, A *J. Mater. Res.* **1997**, *12*, 2759.
(17) Katsumata, K.; Cordonier, C. E. J.; Shichi, T.; Fujishima, A. *J. Am. Chem. Soc.* **2009**, *131*, 3856.
(18) Kudo, A.; Tanaka, A.; Domen, K.; Maruya, K.; Aika, A.; Onishi, T. *J. Catal.* **1988**, *111*, 67.

(19) Domen, K.; Kudo, A.; Shinozaki, A.; Tanaka, A.; Onishi, T. *Catal. Today* **1990**, *8*, 77.
(20) Sayama, K.; Tanaka, A.; Domen, K.; Maruya, K.; Onishi, T. *J. Phys. Chem.* **1991**, *95*, 1345.
(21) Abe, R.; Shinohara, K.; Tanaka, A.; Hara, M.; Kondo, J. N.; Domen, K. *Chem. Mater.* **1997**, *9*, 2179.
(22) Zhang, G.; Gong, J.; Zou, X.; He, F.; Zhang, H.; Zhang, Q.; Liu, Y.; Yang, X.; Hu, B. *Chem. Eng. J.* **2006**, *123*, 59.
(23) Nedjar, R.; Borel, M. M.; Leclaire, A.; Raveau, B. *J. Solid State Chem.* **1987**, *71*, 182.
(24) Sakowski-Cowley, A. C.; Lukaszewicz, K.; Megaw, H. D. *Acta Crystallogr., Sect. B* **1969**, *25*, 851.
(25) Kruczek, M.; Talik, E.; Kania, A. *Solid State Commun.* **2006**, *137*, 469.
(26) Bizeto, M. A.; Faria, D. L. A.; Constantino, V. R. L. *J. Mater. Sci.* **2002**, *37*, 265.
(27) Shiguihara, A. L.; Bizeto, M. A.; Constantino, V. R. L. *Colloids Surf., A.* **2007**, *295*, 123.
(28) Kaifu, N; *Rica Nenpyo (Chronological Scientific Tables)*; National Astronomical Observatory; Maruzen Co., Ltd: Tokyo, 2004; p 485.
(29) Katsumata, K.; Cordonier, C. E. J.; Shichi, T.; Fujishima, A. *Mater. Sci. Eng., B* **2010**; doi:10.1016/j.mseb.2010.01.00.

AM100091F